Received: 13 พ.ค. 2569 **Revised:** 7 มิ.ย. 2569 **Accepted:** 29 มิ.ย. 2569

การจำลองเชิงฟิสิกส์และโครงข่ายประสาทเทียมของสนามไฟฟ้าบนลูกถ้วยฉนวนที่มีการปนเปื้อน

Physics-Based and Neural Network Modeling of Electric Field Distribution on Contaminated Insulators

รติ วงษ์สถาน*, ชนะพล มหาวรรณ, ยศพร จันทร์ทอง และ ธีราวุฒิ กุลธราธีระ
ภาควิชาวิศวกรรมไฟฟ้า คณะวิศวกรรมศาสตร์และเทคโนโลยี มหาวิทยาลัยนอร์ท-เชียงใหม่

Rati Wongsathan*, Chanapol Mahawan, Yodsapon Junthong and Theerawut Kultharatheera
Department of Electrical Engineering, Faculty of Engineering and Technology, North-Chiang Mai University, Chiang Mai, Thailand, 50230
*Corresponding author: rati@northcm.ac.th

บทคัดย่อ

งานวิจัยนี้เสนอแบบจำลองไฮบริดสำหรับวิเคราะห์และพยากรณ์การกระจายสนามไฟฟ้าบนผิวลูกถ้วยฉนวนโพลิเมอร์คอมโพสิท โดยผสานการจำลองเชิงฟิสิกส์ด้วยระเบียบวิธีไฟไนต์เอลิเมนต์ผ่าน COMSOL Multiphysics เข้ากับโครงข่ายประสาทเทียมแบบเพอเซปตรอนหลายชั้น (Multilayer Perceptron Neural Networks, MLPNN) เพื่อพัฒนาแบบจำลองตัวแทนประมาณค่าสนามไฟฟ้าที่มีประสิทธิภาพ แบบจำลองสามมิติถูกพัฒนาสำหรับสภาวะสะอาด ฝุ่นธรรมชาติ มลพิษอุตสาหกรรม และมูลนกเปียก ผลการจำลองพบว่าการเพิ่มค่าการนำไฟฟ้าของชั้นปนเปื้อนส่งผลให้เกิดการบิดเบือนของสนามไฟฟ้าและเพิ่มความเสี่ยงต่อการเกิดการวาบไฟตามผิว โดยกรณีมูลนกเปียกให้ค่าสนามไฟฟ้าสูงสุด 480 kV/m นอกจากนี้ ได้ทำการเปรียบเทียบโครงสร้าง MLPNN จำนวน 26 รูปแบบด้วยวิธี Grid Search พบว่า MLPNN ที่มีสามชั้นซ่อน [5 10 5] ให้สมดุลที่เหมาะสมระหว่างความแม่นยำและความซับซ้อน ข้อมูลจาก COMSOL จำนวน 3,200 ตัวอย่างได้แบ่งออกเป็นข้อมูลชุดฝึกสอนและทดสอบ ในอัตราส่วน 80:20 โดยให้ค่า Test MSE เป็น 0.0287 และ RMSE เป็น 0.1695 และสามารถพยากรณ์สนามไฟฟ้าใกล้เคียง COMSOL แสดงให้เห็นศักยภาพการวิเคราะห์ฉนวนไฟฟ้าแรงสูงและการพัฒนาเครื่องมือประเมินความเชื่อถือได้ของระบบไฟฟ้าในอนาคต

คำสำคัญ : *ลูกถ้วยฉนวนโพลิเมอร์คอมโพสิท; การกระจายสนามไฟฟ้า; การปนเปื้อนบนผิวฉนวน; ระเบียบวิธีไฟไนต์เอลิเมนต์; โครงข่ายประสาทเทียมแบบหลายชั้น*

Abstract

This study proposes a hybrid modeling framework for analyzing and predicting electric field distribution on polymer composite insulators by integrating physics-based finite element simulations in COMSOL Multiphysics with Multilayer Perceptron Neural Networks (MLPNN). Three-dimensional models were developed under clean, natural dust, industrial contamination, and wet bird-dropping conditions. Simulation results revealed that increasing contamination conductivity significantly distorted the electric field distribution and increased flashover risk, with the wet bird-dropping condition producing the highest electric field intensity of 480 kV/m. Furthermore, 26 MLPNN architectures were evaluated using a grid search approach. The MLPNN with three-hidden-layer architecture [5 10 5] achieved the best balance between prediction accuracy and model complexity. A total of 3,200 COMSOL-generated samples were divided into training and testing datasets using an 80:20 ratio. The selected model achieved a test MSE of 0.0287 and an RMSE of 0.1695 while providing electric field predictions closely matching COMSOL results. These findings demonstrate the potential of combining physics-based simulation and neural networks for high-voltage insulation analysis and future power system reliability assessment.

Keywords: *Composite polymer insulator; Electric field distribution; Surface contamination; Finite element method; Multilayer perceptron neural network*

1. Introduction

Electrical insulators are critical components in outdoor power substations and transmission systems, serving to isolate energized conductors and prevent short-circuit faults. Under operating conditions, insulator surfaces are exposed to environmental contaminants. In humid environments, these contaminants may react with atmospheric pollutants and acidic gases, degrading the surface morphology and electrical characteristics of the insulator, which leads to localized electric-field enhancement (Ramos Hernanz et al., 2006). Consequently, the risk of surface flashover and insulation failure increases.

Accurate prediction of electric field distribution on contaminated insulators remains challenging due to complex insulator geometry and nonuniform contamination layers. To address this issue, various analytical and numerical approaches have been proposed. Palangar *et al.* (2019) developed simplified analytical models to reduce computational complexity, while Li Xingcai *et al.* (2025) investigated contamination-induced electric-field distortion using particle-based pollution models. In practical applications, contamination characteristics vary significantly in terms of conductivity, moisture content, and spatial distribution. Arshad *et al.* (2015) modeled contamination as a conductive layer and demonstrated that electric-field intensity increases with contamination conductivity and layer thickness. Their results showed good agreement with experimental observations, confirming the reliability of numerical techniques for contaminated-insulator analysis (Benguesmia *et al*., 2019).

In recent years, artificial intelligence (AI)-based approaches have attracted considerable attention for reducing computational burden while improving modeling capability. Neural networks have demonstrated strong performance in learning nonlinear relationships between contamination conditions and electric-field behavior, with prediction results closely matching FEM simulations (Aydogmus, 2009; Menesy *et al*., 2024). In addition, physics-informed neural networks have been applied for efficient electric-field estimation in two- and three-dimensional domains (Zeng *et al*., 2023).

Motivated by these developments, this study proposes a hybrid framework integrating FEM-based simulation in COMSOL Multiphysics with a multilayer perceptron neural network (MLPNN) to develop a surrogate model for electric field prediction on contaminated insulator surfaces. Although FEM provides high accuracy for complex geometries and physical phenomena, it requires considerable computational time and resources. Therefore, FEM-generated datasets are utilized to train the MLPNN for rapid and efficient electric-field estimation with satisfactory accuracy.

A three-dimensional composite polymer insulator model commonly used in high-voltage distribution systems is investigated under clean condition, natural dust contamination, industrial pollution, and localized wet bird-dropping contamination. The study aims to analyze electric field behavior along the creepage distance, identify high electric-field concentration regions, and evaluate the prediction capability of the proposed MLPNN against FEM simulation results. The proposed framework demonstrates strong potential for high-voltage insulation design and reliability assessment applications.

Despite the considerable progress in FEM-based electric field analysis and AI-based prediction models, several research gaps remain. Most previous studies focused either on numerical simulation or neural-network prediction separately. Furthermore, systematic optimization of MLPNN architectures for contaminated-insulator electric-field estimation has received limited attention. Therefore, this study proposes an integrated FEM–MLPNN framework in which COMSOL-generated datasets are utilized to develop and optimize surrogate neural-network models through a structured grid-search procedure.

2. Theoretical background

Electric field analysis on insulator surfaces can be performed under both direct current (DC) and alternating current (AC) conditions (Meng et al., 2025), depending on the operating environment and surface contamination characteristics.

2.1 DC Electric Field Model

Under DC steady-state conditions, the electric field behaviour can be described using fundamental electrostatic relationships among electric flux density, electric field intensity, and electric potential, as expressed in (1).

$$\left.\begin{aligned} \nabla \cdot \mathbf{D} &= \rho_v \\ \mathbf{E} &= -\nabla V \\ \mathbf{D} &= \varepsilon_0 \varepsilon_r \mathbf{E} \end{aligned}\right\} \quad (1)$$

where **D** is the electric flux density (C/m^2), ρ_v is the volume charge density (C/m^3), **E** is the electric field intensity (V/m), V is the electric potential (V), ε_0 is the permittivity of free space, and ε_r is the relative permittivity of the material.

In the absence of free charge (ρ_v = 0), the governing equation reduces to the Laplace equation:

$$\nabla \cdot (\varepsilon_0 \varepsilon_r \nabla V) = 0 \quad (2)$$

This model is commonly applied to clean-surface conditions, where surface conduction current is negligible. The resulting electric field distribution can therefore be used as a baseline for comparison with contaminated conditions.

2.2 AC Electric Field Model

For AC conditions, both conduction current and displacement current must be considered. The total current density can be expressed as

$$\left.\begin{aligned} \nabla \cdot \mathbf{J} &= Q_j \\ \mathbf{J} &= \sigma \mathbf{E} + \mathbf{J}_e \\ \mathbf{E} &= -\nabla V \end{aligned}\right\} \tag{3}$$

where **J** is the total current density (A/m^2), Q_j is the current source density (A/m^3), σ is the electrical conductivity of the material or contamination layer (S/m), and $\mathbf{J_e}$ is the external current density (A/m^2).

Unlike the DC case, the AC electric field distribution strongly depends on surface conductivity, which varies with contamination severity and moisture content. A thin conductive water film on the insulator surface can increase conductivity, resulting in higher leakage current, electric-field distortion, and increased flashover risk.

3. Methodology

The overall workflow of the proposed FEM–MLPNN framework is illustrated in Fig. 1. The process begins with the development of a three-dimensional composite polymer insulator model, followed by FEM-based electric field simulations in COMSOL Multiphysics to generate electric field data under different contamination conditions. The generated dataset is then pre-processed through normalization and feature selection and subsequently partitioned into training (80%) and testing (20%) datasets. A grid search procedure is employed to investigate 26 candidate MLPNN architectures. The selected networks are trained using the Levenberg–Marquardt backpropagation algorithm and evaluated using MSE and RMSE metrics. Finally, the optimal MLPNN architecture is identified and used as a computationally efficient surrogate model for predicting electric field distributions on contaminated insulator surfaces.

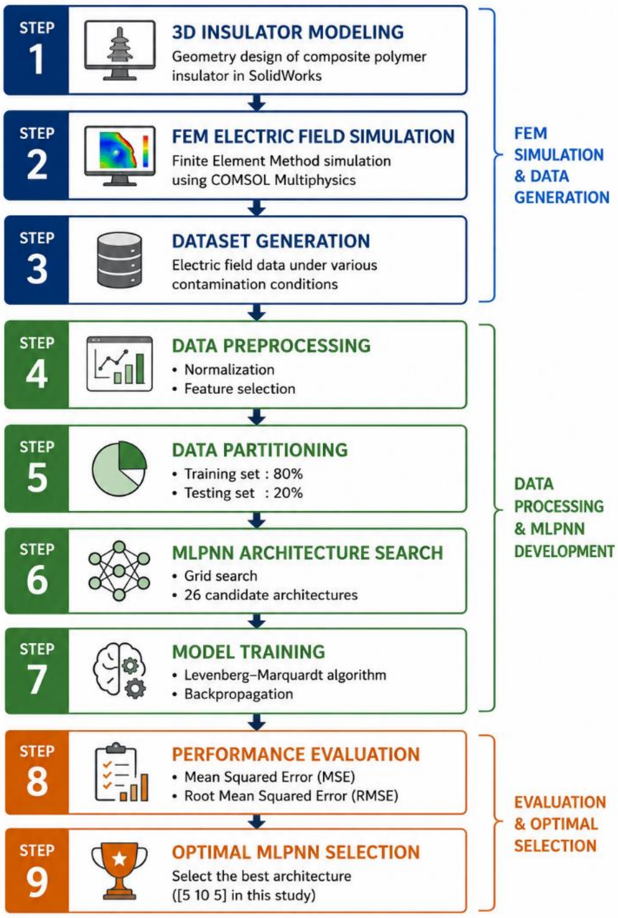

Figure 1 Research workflow of the proposed FEM–MLPNN framework for electric field prediction on contaminated insulator surfaces.

3.1 Electric Field Simulation Using COMSOL Multiphysics

COMSOL Multiphysics version 5.5 (COMSOL AB, 2019) is employed to simulate the electric field distribution. The geometric model of the insulator is first designed in SolidWorks (Fig. 2(a)), and subsequently imported into COMSOL for FEM-based analysis. The computational domain is discretized using a physics-controlled unstructured tetrahedral mesh, as shown in Fig. 2(b). The mesh size is set to the “Finer” level in COMSOL Multiphysics to improve spatial resolution throughout the computational domain. Additional mesh refinement is automatically applied near the insulator sheds and regions with expected electric-field concentration, where high field gradients are likely to occur. This mesh configuration is well suited for representing the curved and geometrically complex structure of composite polymer insulators while maintaining computational efficiency. Within each element, the electric field problem is governed by the Laplace equations in (1) – (3) under specified boundary conditions. The governing equations are transformed into weak form by multiplying with the test function (ω) and integrating over the computational domain (Ω), yielding

$$\int_{\Omega} \varepsilon_0 \varepsilon_r \nabla V \cdot \nabla \omega \, d\Omega = 0 \qquad (4)$$

The resulting element equations are assembled into a large linear algebraic system. The electric field distribution is obtained using the stationary solver available in COMSOL Multiphysics under the specified boundary conditions and material properties. The solver computes the electric potential distribution throughout the computational domain, from which the electric field intensity is derived according to the governing equations presented in Section 2.

The resulting element equations are assembled into a large linear algebraic system and solved numerically using direct or iterative solvers. The electric field distribution at each location is then obtained from the potential gradient relationship in (1) as illustrated in Fig. 2(c).

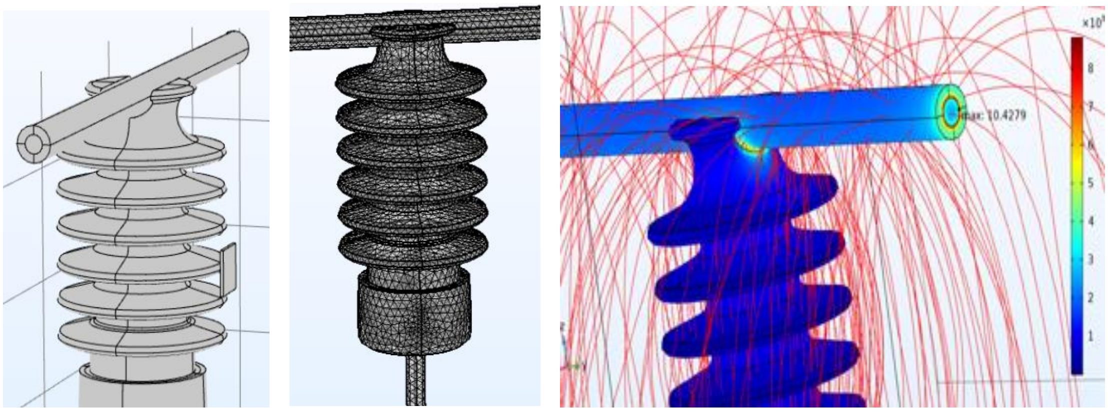

(a) (b) (c)

Figure 2 (a) Geometric modeling of the insulator in SolidWorks, (b) Tetrahedral mesh structure of the insulator model, and (c) Electric field distribution and electric field lines around the insulator obtained from COMSOL Multiphysics simulation.

After assigning the electrical properties (ε_r, σ) to the insulator. Surface contamination is modeled as an additional layer with different electrical characteristics. Clean and natural pollution conditions are defined with low $\sigma \sim 10^{-6}$ S/m and $\varepsilon_r \approx 3$, whereas industrial pollution exhibits by higher $\sigma \sim 10^{-3}$ S/m and $\varepsilon_r \approx 8$. Wet bird-dropping condition represents the highest contamination severity, with $\sigma \sim 1$ S/m and $\varepsilon_r \approx 70$. Dirichlet voltage and grounded boundary conditions are applied to represent practical operation. Locally refined meshes are generated near the insulator surface and expected electric-field concentration regions to improve numerical accuracy. The FEM simulations then produce electric field distributions, which are subsequently used as training data for the proposed MLPNN surrogate models.

3.2 Development of the MLPNN for Electric Field Estimation

In this study, MLPNN is developed as a surrogate model for estimating electric field distribution on contaminated insulator surfaces. The training dataset is obtained from FEM-based COMSOL simulations, which are computationally intensive and time-consuming. Therefore, the simulated data are utilized to train the MLPNN. A total of 3,200 simulation samples are generated from COMSOL Multiphysics under different combinations of insulator properties, contamination conditions, and operating voltages. The MLPNN model is developed and trained using MATLAB R2024a Neural Network Toolbox on a personal computer equipped with an Intel Core i7 processor and 16 GB RAM.

The proposed MLPNN architecture (Fig. 3) is designed to learn the nonlinear relationship between system parameters and electric field behaviour. The model employs nine input variables representing insulator material properties, contamination characteristics, and operating conditions, including relative permittivity of the insulator (ε_r), insulator conductivity (σ_{ins}), contamination type (C_{type}), contamination conductivity (σ_{cont}), contamination relative permittivity ($\varepsilon_{r,cont}$), contamination thickness (t_{cont}), applied voltage (V), insulator length (L), and creepage-distance position (x). The output variable is the electric field intensity (E_{field}) obtained from COMSOL simulations, which serves as the ground-truth target for model training. As illustrated in Fig. 3, the input layer consists of nine neurons corresponding to the selected input variables. The hidden layers employ the rectified linear unit (ReLu) activation function to capture nonlinear relationships among the input parameters, whereas the output layer uses a linear activation function (purelin) to predict the continuous electric field value. The input layer performs data transfer without applying an activation function.

The hidden-layer configuration of the MLPNN is systematically determined using a constrained grid-search approach rather than trial-and-error selection. The number of neurons in each hidden layer is selected from the set {1, 2, 5, 10}, while the network depth ranges from one to four hidden layers. Instead of evaluating all possible combinations, 26 representative architectures are selected to cover shallow, moderate, and deep neural network structures while maintaining a balance between prediction accuracy and training complexity. The investigated architectures include single-hidden-layer structures such as [1], [2], and [10] as baseline models; two-hidden-layer structures such as [5 5] and [10 10] for shallow-network evaluation; three-hidden-layer structures such as [10 10 5]; and deeper architectures including [5 10 5 2] and [10 10 10 5] to investigate the influence of network depth on prediction performance.

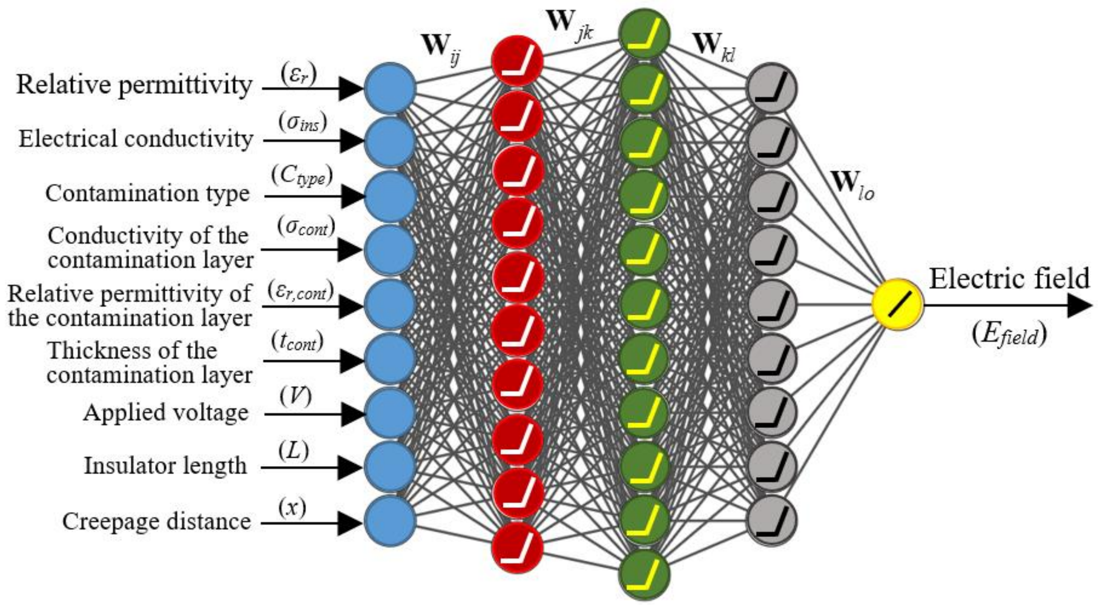

Figure 3 Architecture of the multilayer perceptron neural network (MLPNN) for predicting electric field distribution on contaminated insulator surfaces.

For each architecture, the MLPNN model is trained using preprocessed and normalized datasets. The training process employs the Levenberg–Marquardt optimization algorithm because of its fast convergence and superior performance for medium-sized regression problems compared with conventional gradient-descent methods. Model performance is evaluated using MSE and RMSE on the testing dataset. The prediction performance of all candidate architectures is subsequently compared to identify the most suitable network configuration. This systematic approach reduces the bias associated with trial-and-error parameter selection and provides a more reliable basis for selecting an optimal architecture.

Prior to training, all input variables are normalized using the StandardScaler technique to obtain zero mean and unit standard deviation, thereby reducing scale imbalance among variables. The dataset contains 3,200 samples, of which 80% (2,560 samples) are used for training and 20% (640 samples) are used for testing. The dataset is divided using a random state of 42 to ensure reproducibility. The MLPNN models are trained for 500 epochs using the backpropagation algorithm (BPA). Full-batch training is adopted without mini-batch partitioning to improve training stability using the entire dataset in each epoch.

4. Results and Discussion

4.1 Electric Field Distribution on Contaminated Insulator Using COMSOL

The simulated electric field distributions along the creepage distance of the composite polymer insulator under clean condition, natural dust contamination, industrial pollution, and wet bird-dropping contamination are shown in Figs. 4–7. In all cases, the maximum electric field occurs near the high-voltage and grounded terminals due to geometric field crowding.

Under clean conditions, the electric field distribution is relatively uniform, with most values ranging from 60–120 kV/m and a peak value of approximately 420 kV/m near the high-voltage terminal. The grounded side exhibits values around 250 kV/m, indicating low surface leakage current. Under natural dust contamination, the field profile remains similar but exhibits slight ripples along the shed geometry, with electric field intensity increasing to approximately 70–130 kV/m and a peak value of about 430 kV/m. Industrial pollution causes significant electric-field distortion and multiple local field spikes due to charge accumulation and increased surface leakage current. The intermediate electric field ranges from 60–140 kV/m, while the maximum value increases to approximately 450 kV/m, indicating higher localized electrical stress and flashover risk. In contrast, wet bird-dropping contamination produces the most severe condition due to the formation of a conductive moisture film on the insulator surface. The electric field intensity in the middle region increases to approximately 70–150 kV/m, with a maximum value of about 480 kV/m, representing the highest flashover and insulation degradation risk among all investigated conditions.

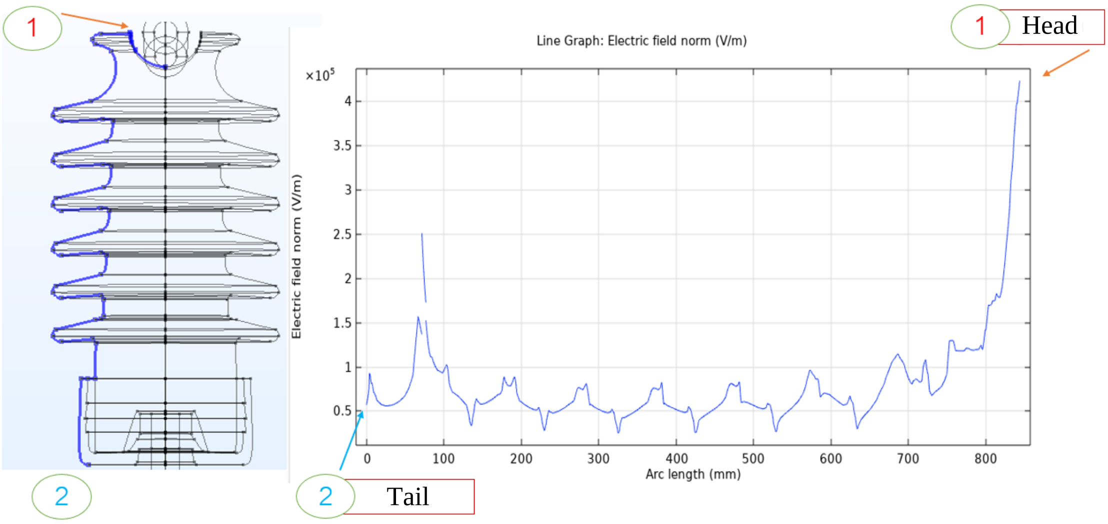

Figure 4 Electric field distribution along the creepage distance on the insulator surface under clean condition.

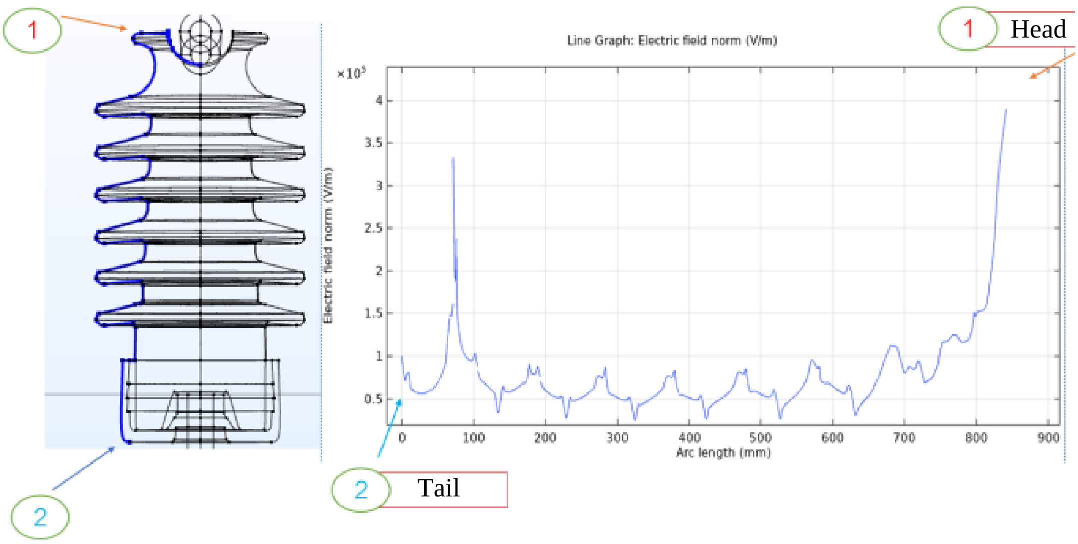

Figure 5 Electric field distribution along the creepage distance on the insulator surface under natural dust condition.

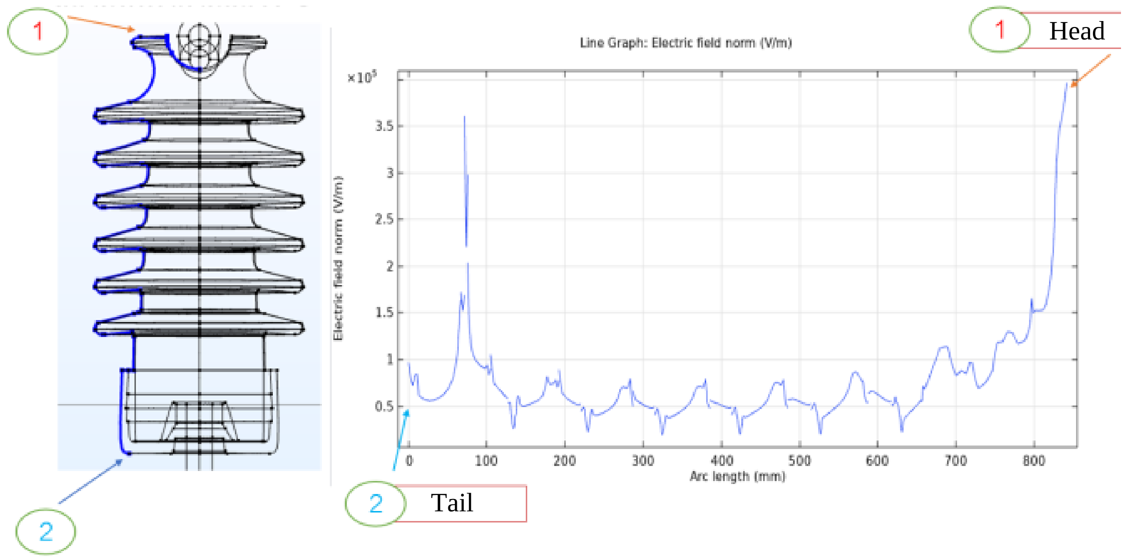

Figure 6 Electric field distribution along the creepage distance on the insulator surface under industrial pollution condition.

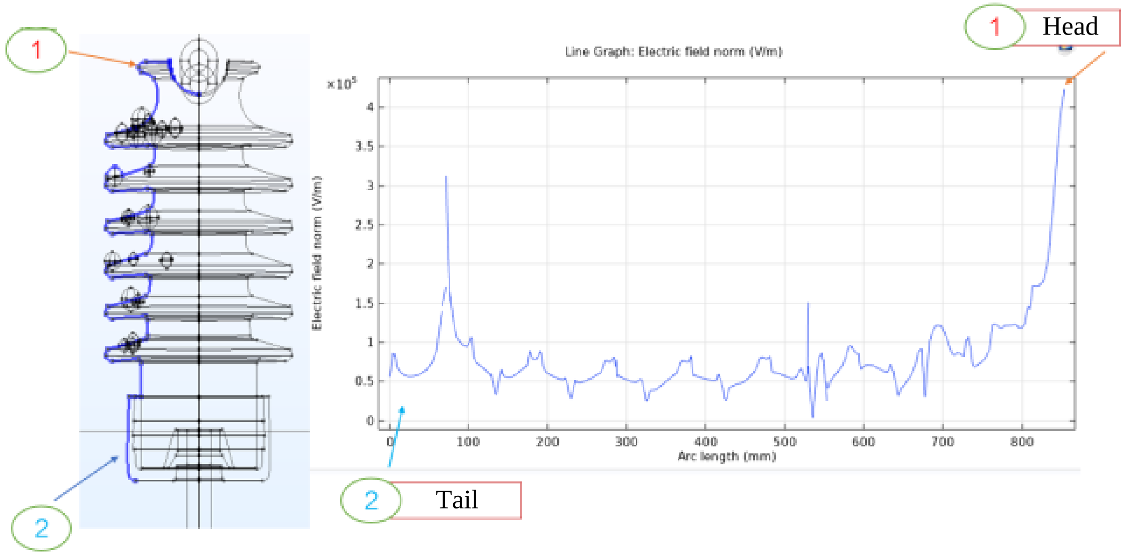

Figure 7 Electric field distribution along the creepage distance on the insulator surface under wet bird-dropping contamination condition.

As summarized in Table 1, the maximum electric field intensity increases with contamination severity. Wet bird-dropping contamination produces the highest electric field intensity of 480 kV/m, corresponding to a 14.29% increase compared with the clean condition. In contrast, natural dust contamination causes only a slight increase of 2.38%, indicating a relatively minor influence on the electric field distribution.

Table 1 Summary of maximum electric field intensity under different contamination conditions.

Conditions	Maximum E (kV/m)	Increase (%)
Clean	420	0
Natural Dust	430	2.38
Industrial Pollution	450	7.14
Wet Bird Dropping	480	14.29

The observed electric-field enhancement under industrial pollution and wet bird-dropping contamination is consistent with the findings reported by Arshad et al. (2015), who demonstrated that increasing contamination conductivity increases surface leakage current and field distortion. The present results also support the theoretical current-density relationship described in (3), where higher conductivity contributes to stronger conductive current paths and localized electric-field concentration. Consequently, contamination layers with higher conductivity produce more severe electric-field distortion and increase the risk of insulation degradation and surface flashover.

4.2 MLPNN Architecture Design for Electric Field Prediction

The COMSOL results in Section 3.1 are used to develop the MLPNN model for electric field estimation along the creepage distance. The architecture selection results in Table 2 and Fig. 8 show that medium- and large-scale networks consistently achieve Test MSE values below 0.05. Among all architectures, [10 10 5] produces the lowest Test MSE and Test RMSE, followed closely by [10 10 10 5]. However, [5 10 5] achieves prediction errors within 3% of the best model while using only 20 neurons, compared with 25 and 35 neurons for [10 10 5] and [10 10 10 5], respectively. The close Train MSE and Test MSE values of [5 10 5] also indicate good generalization capability. In contrast, smaller architectures such as [5] and [5 5] produce significantly higher Test MSE values, indicating limited capability in learning nonlinear system behavior, while deeper architectures provide only marginal improvement.

Table 2 MLPNN architecture selection results using the grid-search method.

No.	Structure*	Train MSE	Test MSE	Test RMSE	No.	Structure*	Train MSE	Test MSE	Test RMSE
1	[1]	0.74489	0.93893	0.96898	14	[1 2 1]	0.97836	1.0807	1.0396
2	[2]	0.45856	0.47759	0.69108	15	[2 2 2]	0.13356	0.1305	0.36124
3	[5]	0.069128	0.058464	0.24179	16	[2 5 2]	0.29515	0.34875	0.59055
4	[10]	0.038117	0.046061	0.21462	17	[5 5 2]	0.056565	0.063439	0.25187
5	[1 1]	0.97836	1.0807	1.0396	18	[5 5 5]	0.041533	0.058248	0.24135
6	[1 2]	0.54771	0.61033	0.78124	19	[5 10 5]	0.020498	0.028728	0.16949
7	[2 2]	0.97836	1.0807	1.0396	20	[10 5 2]	0.23566	0.30541	0.55264
8	[2 5]	0.046723	0.055345	0.23525	21	[10 10 5]	0.02116	0.027869	0.16694
9	[5 2]	0.27259	0.33486	0.57867	22	[1 2 2 1]	0.46216	0.46830	0.68432
10	[5 5]	0.035855	0.041912	0.20473	23	[2 5 5 2]	0.97836	1.0807	1.0396
11	[5 10]	0.045452	0.066406	0.25769	24	[5 5 5 5]	0.23744	0.32471	0.56983
12	[10 5]	0.025498	0.033818	0.18390	25	[5 10 5 2]	0.03662	0.039484	0.19871
13	[10 10]	0.023187	0.030377	0.17429	26	[10 10 10 5]	0.019416	0.028153	0.16779

Note: *The notation inside [ ] represents the hidden-layer architecture of the MLPNN, where each number denotes the number of neurons in each hidden layer. For example, [1] indicates one hidden layer with one neuron, [5 10] denotes two hidden layers with 5 and 10 neurons, respectively.

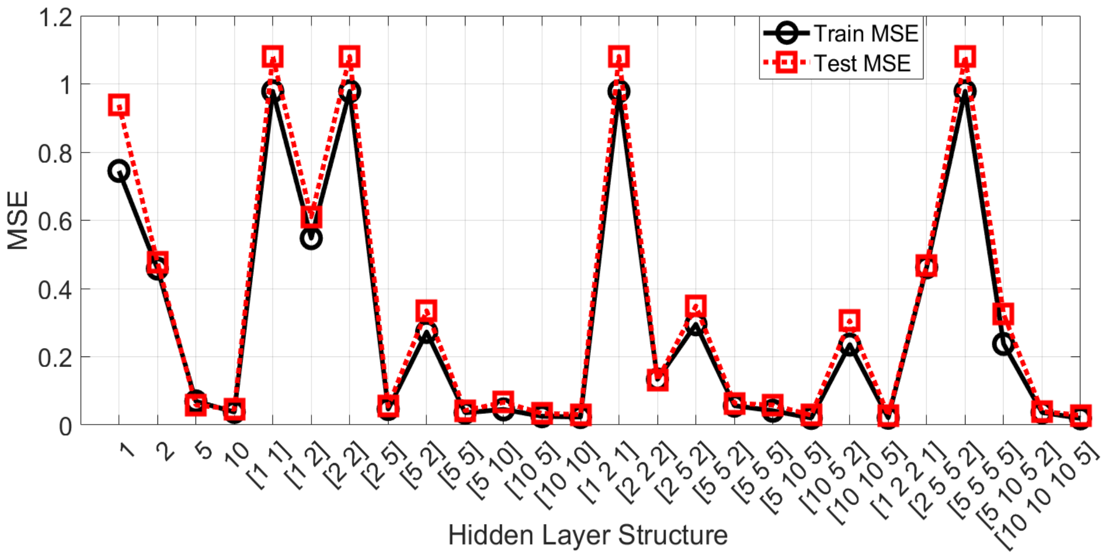

Figure 8 Training and testing MSE values for different MLPNN architectures.

The [5] architecture contains 56 trainable parameters (50 weights and 6 biases) with computational complexity ~ $O(50)$, whereas [5 10 5] requires 171 parameters (150 weights and 21 biases) with complexity ~ $O(150)$ per sample, where $O(\cdot)$ denotes computational complexity order. Although [5] requires lower computational cost, its prediction errors remain substantially higher. Therefore, [5 10 5] is selected because it reduces prediction error by approximately 50% compared with [5] while maintaining a suitable balance between prediction accuracy and model complexity.

4.3 Electric Field Prediction on Contaminated Insulator Surfaces Using MLPNN

The simulation results in Fig. 9 compare the prediction capabilities of MLPNN[5] and MLPNN[5 10 5] for estimating electric field distribution along the creepage distance. Both architectures capture the overall field trend, with high electric field intensity near the beginning and end of the creepage path and lower values in the middle region. However, MLPNN[5 10 5] produces predictions that are closer to the FEM-based COMSOL results, particularly in regions with rapid field variation and local peaks.

As shown in Fig. 9(a), MLPNN[5] approximates the general field trend but exhibits noticeable deviations near high-field regions and cannot accurately track localized fluctuations due to its limited network capacity. In contrast, MLPNN[5 10 5] in Fig. 9(b) provides more accurate electric field predictions across all contamination conditions, especially in the intermediate creepage region around 330–350 mm, where different contamination levels are more clearly distinguished. These results confirm that the deeper MLPNN architecture provides superior capability in learning nonlinear electric field behavior and contamination-dependent characteristics.

Furthermore, in Fig. 9(c), MLPNN[5] exhibits relatively wide data dispersion around the reference line, particularly above 150 kV/m, where noticeable deviations occur near local field peaks. This indicates limited capability in learning nonlinear electric field characteristics and reduced generalization performance in the medium- and high-field regions. In contrast, Fig. 9(d) shows that the predictions of MLPNN[5 10 5] are more tightly clustered around the reference line across the entire electric field range, including values exceeding 300 kV/m. The narrower distribution and reduced outliers indicate improved learning capability for the nonlinear relationship between system parameters and electric field behavior. These observations are consistent with the lower Test MSE (0.0287) and Test RMSE (0.1695) values of MLPNN[5 10 5], confirming its superior accuracy and stability for electric field estimation on contaminated insulator surfaces.

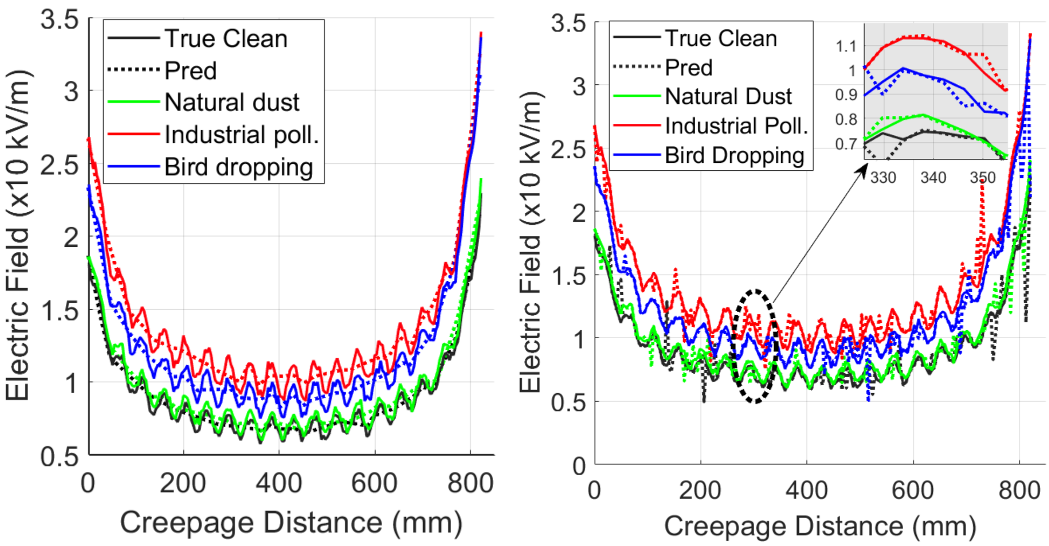

(a) MLPNN[5] (b) MLPNN [5 10 5]

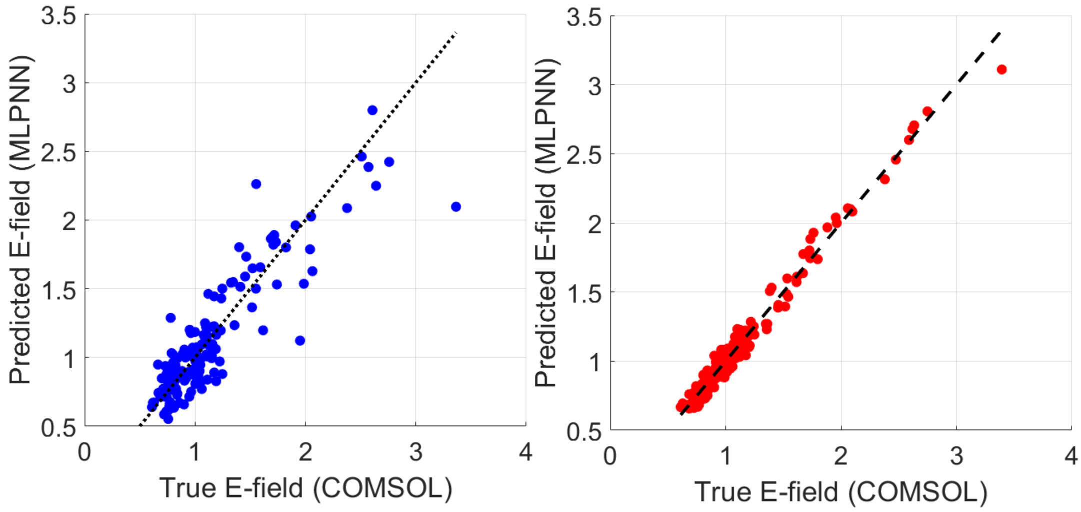

(c) (d)

Figure 9 Comparison of electric field prediction along the creepage distance and corresponding true-versus-predicted electric field results for (a) and (c) MLPNN[5], and (b) and (d) MLPNN[5 10 5] under different contamination conditions.

The superior performance of MLPNN[5 10 5] can be attributed to its greater representational capacity, which enables the network to capture the highly nonlinear relationship between contamination characteristics, operating conditions, and electric field distribution. In contrast, the simpler MLPNN[5] architecture contains fewer trainable parameters and therefore exhibits limited capability in representing localized field variations and sharp electric-field gradients. These findings are consistent with previous studies on neural-network-based electric field prediction, which reported that appropriately selected multilayer architectures provide improved approximation accuracy for complex electromagnetic problems.

From an engineering perspective, the proposed MLPNN surrogate model significantly reduces the computational burden associated with repeated FEM simulations while maintaining satisfactory prediction accuracy. This capability is particularly beneficial for rapid condition assessment, optimization studies, and future real-time monitoring applications involving contaminated high-voltage insulators.

5. Conclusion

This study proposes a hybrid FEM–MLPNN framework for modeling and predicting electric field distribution on contaminated composite polymer insulators. The results demonstrate that contamination severity significantly influences electric field distortion, with wet bird-dropping contamination producing the highest electric field intensity and flashover risk. Among the investigated neural-network architectures, MLPNN[5 10 5] provides the most suitable balance between prediction accuracy and model complexity, achieving stable prediction performance and good generalization capability across different contamination conditions. The main contribution of this work lies in the integration of physics-based FEM simulations with data-driven MLPNN surrogate modeling for rapid electric field estimation. Unlike conventional FEM analysis, which requires repeated numerical computation, the proposed surrogate model provides comparable prediction capability with substantially reduced computational burden. From a practical perspective, the proposed framework can support rapid insulation-condition assessment, design optimization, and future intelligent monitoring systems for contaminated high-voltage insulators. The developed methodology also provides a foundation for future AI-assisted diagnostic and predictive maintenance applications in power transmission and distribution systems.

5.1 Limitations of the Study

The present study is limited to simulation-based analysis under static contamination conditions. The contamination layers are represented by equivalent electrical properties and do not account for temporal variations in humidity, rainfall, contamination accumulation, or other environmental factors that may influence electric field behavior under practical operating conditions. In addition, the proposed MLPNN models are trained using FEM-generated datasets and have not yet been validated using experimental measurements.

5.2 Future Research Directions

Future work will focus on experimental validation, dynamic contamination modelling, and transient electric-field analysis under time-varying environmental conditions. Additional contamination types, including marine salt fog, agricultural or fertilizer pollution, mixed wet-layer contamination, carbon dust, cement dust, and oil or hydrocarbon contamination, should also be investigated. Furthermore, the proposed framework can be extended to other insulator materials, such as porcelain and glass insulators, to evaluate material-dependent electric field characteristics and contamination performance under realistic operating environments. The integration of MLPNN-based surrogate models with real-time monitoring and condition assessment systems also represents a promising direction for future research.

6. References

Arshad, A., Nekahi, A., McMeekin, S. G., & Farzaneh, M. (2015). Effect of pollution layer conductivity and thickness on electric field distribution along a polymeric insulator. Proceedings of the COMSOL Conference 2015, Grenoble, France, 1–4.

Aydogmus, Z. (2009). A neural network-based estimation of electric fields along high voltage insulators. *Expert Systems with Applications, 36*(5), 8705–8710. https://doi.org/10.1016/j.eswa.2008.11.030

Benguesmia, H., Bakri, B., Khadar, S., Hamrit, F., & M'ziou, N. (2019). *Experimental study of pollution and simulation on insulators using COMSOL® under AC voltage*. *Diagnostyka*, 20(3), 1–5. https://doi.org/10.29354/diag/110330

COMSOL AB. (2019). *COMSOL Multiphysics® (Version 5.5) [Computer software].* COMSOL AB. https://www.comsol.com

Li, X., Liu, Y., & Wang, J. (2025). Influence of surface contamination on electric field distribution of insulators. Chinese Physics B, 34(3), 034101.

Menesy, A. S., Kotb, K. M., Ali, M., Zayed, M. E., Habiballah, I. O., & Abido, M. A. (2024). Enhanced analysis of electric field distribution in high voltage insulators using advanced ANN. Proceedings of the IEEE Sustainable Power and Energy Conference (iSPEC), 428–432. https://doi.org/10.1109/iSPEC59716.2024.10892607

Meng, X., Lin, L., Li, H., Mei, H., & Wang, Z. (2025). Influence of intense vertical component electric field with the direction away from insulation surface on streamer discharge. *IEEE Transactions on Dielectrics and Electrical Insulation, 32*(3), 1712–1718. https://doi.org/10.1109/TDEI.2024.3452652

Palangar, M., Faramarzi, M., & Mirzaie, M. (2019). Improved mathematical model of polluted insulators nonlinear behaviour under AC voltage based on experimental tests. *Characterization and Application of Nanomaterials, 2*(1), 1-9. https://doi.org/10.24294/can.v2i1.541

Ramos Hernanz, J. A., Campayo Martín, J. J., Gogesascoechea, J. M., & Zamora Belver, I. (2006). *Insulator pollution in transmission lines*. *Renewable Energy & Power Quality Journal*, **1**(4), 124–130. https://doi.org/10.24084/repqj04.256

Zeng, X., Zhang, S., Ren, C., & Shao, T. (2023). Physics-informed neural networks for electric field distribution characteristics analysis. *Journal of Physics D: Applied Physics, 56*, acbec3. https://doi.org/10.1088/1361-6463/acbec3